THE JOURNAL OF PHYSICAL CHEMISTRY B

© Copyright 2004 by the American Chemical Society VOLUME 108, NUMBER 9, MARCH 4, 2004

LETTERS

Electrochemical Growth of Three-Dimensional Nanostripe Architecture of Antimony on Cu(100)

Ji-Hong Wu,[†] Jia-Wei Yan,[†] Zhao-Xiong Xie,[†] Qi-Kun Xue,[‡] and Bing-Wei Mao*,[†]

State Key Laboratory for Physical Chemistry of Solid Surfaces and Chemistry Department, Xiamen University, Xiamen 361005, China, and State Key Laboratory for Surface Physics, Institute of Physics, The Chinese Academy of Sciences, Beijing 100080, China

Received: September 13, 2003; In Final Form: December 7, 2003

We report the electrochemical growth of a well-oriented 3D nanostripe architecture of Sb on Cu(100), the system of which has a large crystallographic misfit but still shows thickness-independent growth features. A coincidence between Sb and Cu(100) occurs with $5 \times d_{Sb[110]} = 6 \times d_{Cu[0\bar{1}0]}$ and $d_{Sb[1\bar{1}0]} = 2 \times d_{Cu[001]}$. Two observed factors are credited to the formation of periodically separated 2D arrays of ~1-nm-wide nanostripes in the nanostructure; they are the high number of coincidences in Sb[$1\bar{1}0$] as well as the discontinuity of coincidence lattices in Sb[110] formed to release the residual misfit. The vertical alignment of the nanostripes is achieved following the layer-by-layer epitaxy of nanostripes, leading to the formation of a thick nanostripe film with regular straw-mat-type stacking.

An atomistic understanding of thin film growth is of utmost importance in providing guidelines for tailoring surface nanostructures.[1,2] Two-dimensionally ordered nanostructures have been formed utilizing surface dislocations and anisotropy[3,4] or through strain release in heteroepitaxy.[5] An important yet challenging aspect along this direction is the growth of an ordered 3D nanoarchitecture, which is essential for the construction of, for example, photonic crystals.[6] One of the major difficulties in 3D nanostructuring through film growth lies in the misalignment of 2D nanostructures in the vertical direction during further growth. Here, we report the electrochemical growth of a well-oriented 3D nanostripe architecture of Sb on Cu(100) by a coincidence lattice as well as by the layer-by-layer stacking mechanism.

Antimony is an important element in both fundamental research and practical applications. For example, modifying surfaces with a controlled amount of Sb has been found to promote the layer-by-layer growth mechanism of thin film formation[7] and also the efficient oxidation of small organic molecules that are important in fuel cell research.[8] In addition, Sb is an important component in forming III−V antimony-based semiconductor materials that are valuable in electronics and optoelectronics[9] as well as in forming thermoelectric materials.[10]

Antimony is a semimetal with sp^3 hybridization and has a room-temperature-stable rhombohedral crystal structure that shows a large mismatch with the fcc Cu(100) substrate. This contrasts with most metal heteroepitaxy systems wherein the substrate and overgrown metal possess similar crystal structures and bonding characteristics.[11] The directional bonding tendency of Sb has been shown to furnish an Sb_4 molecular precursor in its vapor deposition[12] and to relax the herringbone reconstruction of Au(111) during its submonolayer deposition in an electrochemical environment.[13] However, it has been shown that Sb can form an open-structured superlattice on Cu(100) through underpotential deposition (UPD),[14] which reveals that the adhesion to the Cu substrate is stronger than the cohesive interaction of Sb adatoms. Therefore, heteroepitaxy is possible for this system, but a simple epitaxial relationship would not be expected. Moreover, the variation of metal ion precursors

* Corresponding author. E-mail: bwmao@xmu.edu.cn.
[†] State Key Laboratory for Physical Chemistry of Solid Surfaces and Xiamen University.
[‡] State Key Laboratory for Surface Physics.

10.1021/jp0367326 CCC: $27.50 © 2004 American Chemical Society
Published on Web 02/05/2004

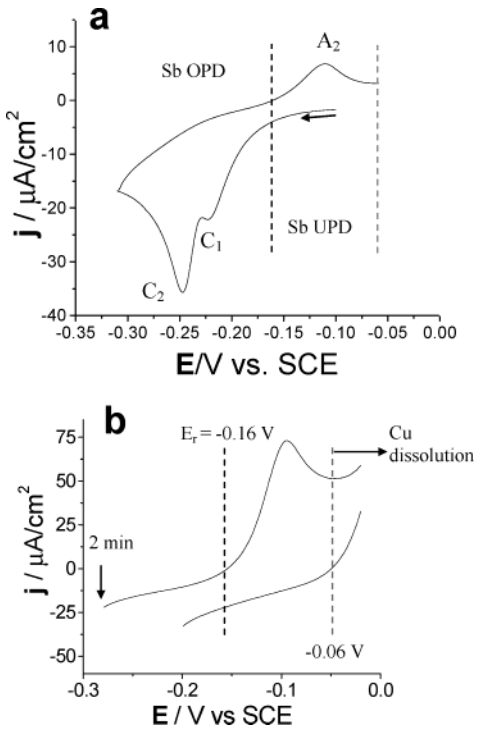

Figure 1. (a) Cyclic voltammograms of Sb electrodeposition on Cu(100) electrodes. (b) Anodic stripping curves recorded after resting at −0.28 and −0.2 V, respectively, for 2 min. Solution: 0.1 mM Sb(III) + 10 mM H_2SO_4. Sweep rate: (a) 5 mV/s, (b) 10 mV/s.

as well as coadsorption processes occurring in electrolytes may also accommodate its electrodeposition in an unique way.[15] However, the growth behavior of semimetallic elements such as Sb and Bi seem to be overlooked in this field. For Sb, only a limited number of in situ and ex situ studies that focus primarily on the superlattice structure of Sb monolayers formed by UPD have been reported.[13,14,16]

In this letter, we report the formation of monatomic-high nanostripes of Sb on Cu(100) and the thickness-independent epitaxy of these nanostripes, which provide a way for the electrochemical growth of an ordered 3D nanoarchitecture from dissimilar materials with a large lattice misfit.

Antimony was electrochemically deposited from dilute sulfuric acid solution containing a low concentration of Sb(III) species prepared by dissolving Sb_2O_3 in sulfuric acid. SbO^+, the predominant form of Sb(III), is in equilibrium with other Sb(III) species depending on the acidity of the solution.[17] In situ STM measurements (Nanoscope IIIa, Digital Instruments) were performed in constant-current mode with electrochemically etched and well-insulated W tips. Typically, an in-situ STM experiment starts with a supporting electrolyte followed by injecting several drops of Sb(III) solution to make the final concentration ranging from 2 to 100 μM in the STM cell. Prior to each experiment, the Cu(100) single-crystal surface was electrochemically polished in 50% phosphoric acid at 2.1 V (vs Pt wire) for 30−40 s followed by thorough rinsing with ultrahigh purity water (Milli-Q). A saturated calomel electrode (SCE) and a platinum wire quasi-reference (~0.5 V vs SCE) were used as the reference electrodes for the electrochemical and in situ STM measurements, respectively. Potentials quoted in this work were normalized to the values against SCE.

The overall behavior of Sb electrodeposition on Cu(100) is characterized by two cathodic processes marked C_1 and C_2 on the cyclic voltammogram (CV) shown in Figure 1a. According to the equilibrium potential for Sb bulk deposition (−0.16 V),

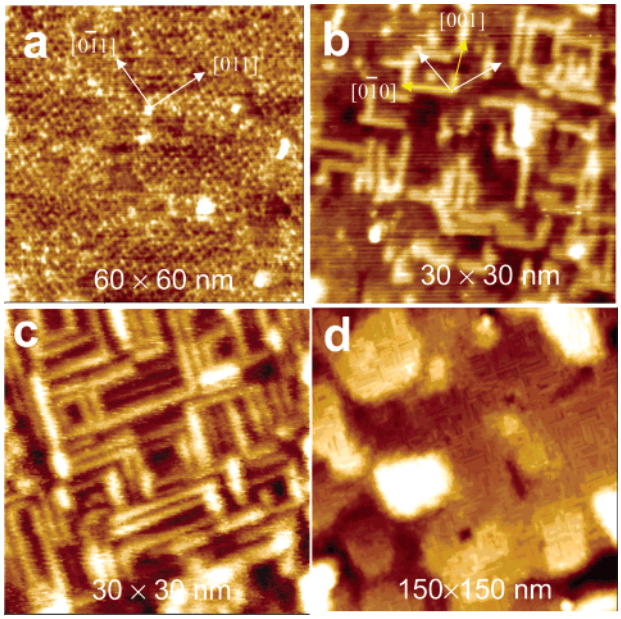

Figure 2. In situ STM images of a (4 × 4) Sb superlattice at −0.26 V (a) and the growth of Sb nanostriptes at −0.32 V (b) on Cu(100) taken in a solution containing 15 μM Sb(III) + 10 mM H_2SO_4. Images c and d were taken in a solution containing 40 μM Sb(III) + 10 mM H_2SO_4.

determined from the anodic stripping curves shown in Figure 1b, peaks C_1 and C_2 correspond to the UPD and overpotential deposition (OPD) of Sb, respectively. The UPD process is kinetically hindered so that it initiates in the UPD region but extends into the OPD region. Although the severe overlapping of the UPD and OPD processes is not typical in electrodeposition, the same has also been observed by Ward et al. in the same system.[14] Because the potential limit of Cu dissolution is located at −0.06 V (Figure 1b), the stripping of UPD Sb is not observed before Cu dissolution, and peak C_1 appeares only in the first cycle of the CV. The voltammetric behaviors are similar to that reported by Ward et al.[14]

The narrow potential window (~100 mV) for Sb UPD posed a difficulty in performing CV in the underpotential region. In situ STM measurements showed, however, that the growth of bulk Sb was kinetically hindered and that its rate was sufficiently low in an extremely dilute Sb(III) solution (e.g., ~2 μM). This facilitated the characterization of a stable (4 × 4) superlattice of a UPD Sb adlayer in an overpotential region as shown by Figure 2a. A few bright spots were formed after the addition of a more concentrated Sb(III) solution (vide infra). The (4 × 4) superlattice with a lattice constant of 1.02 nm is believed to be stabilized by the induced adsorption of sulfates (and/or bisulfates). This was verified by the lack of structures in either pure sulfuric acid solution alone or in perchloric acid media containing Sb(III) species.

The bulk deposition of Sb became obvious when the Sb(III) concentration was increased to 15 μM or higher, as seen by bright spots in Figure 2a from randomly formed nuclei (vide infra); this developed into anisotropic nanostripes along either of the two $\sqrt{2}$ directions of Cu(100) as shown in Figure 2b. The nanostripes are confined to the atomic height and to a width of 1.0 ± 0.1 nm with a typical length of 5−10 nm. These growth characteristics were maintained during the thickening of the deposit until the solution was depleted of Sb(III). This leads to the formation of an Sb nanostripe architecture exhibiting a regular straw-mat type of stacking shown by Figure 2c and d. A thickness of ~5 nm can be reached in a 40 μM Sb(III) solution in the STM cell (~0.5 mL); that is the equivalent of

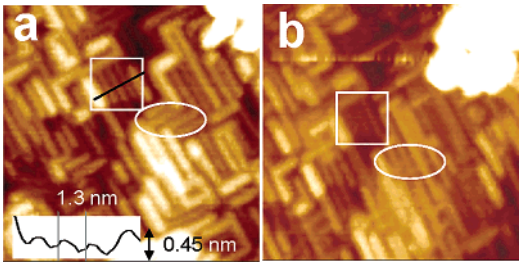

Figure 3. In situ STM images showing the stability of nanostripes at −0.28 V. Frames a and b were recorded at an interval of 7 min. A cross-sectional profile is given to show that nanostripes are evenly separated with monatomic height. The solution is the same as in Figure 2c and d. Scan size: 30 × 30 nm^2.

~20 atomic layers in height. The majority of the nanostripes are evenly separated with an atomic gap of ~0.4 nm. Atomic resolution images were not achieved on these nanostripes. The growth of nanostripes was observed on Cu(100) but not on Cu(111) for Sb(III) concentrations of up to ~100 μM in sulfuric acid or perchlorate acid solutions of 10 mM−0.5 M and at an overpotential larger than 100 mV. Similar perpendicularly oriented needles and high-aspect-ratio domains of atoms were reported previously at the start of the overpotential deposition of tellurium on Au(100), but no further growth behavior was studied.[18]

Investigations of the stability of Sb nanostripes reveal that the Sb nanostripes run exclusively in two perpendicular directions from each other as well as with respect to the next underlayer of nanostripes. As shown in Figure 3a, the majority of these nanostripes grow parallel along the orientation of the next underlayer of nanostripes as indicated by the line in the square. A few of them run across several nanostripes of the next underlayer as indicated in the lines in the ellipse. For these cross-stacking nanostripes, most of them are unstable and would disappear in time. The remainder of the disappearing cross-stacked nanostripes is faintly seen within the lines in the ellipse in Figure 3b. It is anticipated that all of the nanostripes in the film would be parallel stacked at the thermodynamic equilibrium state assuming a layer-by-layer stacking manner.

The invariance of the width and orientation on the thickness of the Sb deposit distinguishes these nanostripes from buckling stripes that are frequently observed in heteroepitaxy when film coherence breaks down up to several layers.[19] Although the fundamentals of nanostripe growth for this system have yet to be fully understood, we believe that the covalent bonding tendency and the layered structure of the rhombohedral α-Sb play major roles in forming the 3D nanostripe architecture. We wish to explain the formation of the nanostripes by alignment with the substrate within the framework of a "coincidence" lattice,[20] a concept that has been developed to explain the heteroepitaxy of large-misfit systems.[21] A perfect coincidence between an epilayer lattice (a_e) and a substrate lattice (a_s) would occur when $n \times a_e = m \times a_s$, where m and n are integers.[21]

The rhombohedral α-Sb (R-3m(166)) has a lattice constant of 4.501 Å. Its equivalent hexagonal crystal structure has lattice parameters of $a_{hex} = 4.30$ Å and $h_{hex} = 11.26$ Å with $Z = 6$ and the nearest atomic distance of 2.91 Å, forming an ABCABC... stacking. An overlay (Figure 4b) shows the (001) plane of Sb in the hexagonal coordination, which comprises two identical hexagonal lattices (the hollow circle slightly above the solid circles). Each Sb atom has three closest-coordinated Sb atoms within a layer. The spacings in the [110] and [1$\bar{1}$0] directions are 2.15 and 3.72 Å, respectively. In the Sb[110] direction, five Sb lattice planes ($5 \times d_{Sb[110]} = 10.75$ Å) match

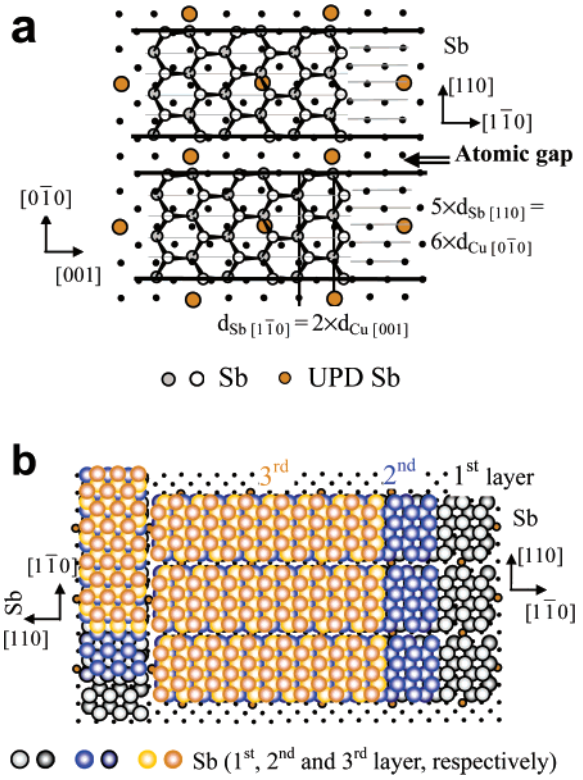

Figure 4. (a) Structural model showing the coincidence lattice sites occurring between Sb and Cu. (b) Parallel stacking of nanostripes on a Cu(100) network. (The larger filled circles represent the locations of Sb atoms from the (4 × 4) superlattice to guide the direction, which may not necessarily be present because they could have been involved in the growth of the nanostripes.)

well with six Cu lattice planes ($6 \times d_{Cu[0\bar{1}0]} = 10.82$ Å) with a deviation parameter of $f_{[110]} = (5 \times d_{Sb[110]} - 6 \times d_{Cu[0\bar{1}0]})/6 \times d_{Cu[0\bar{1}0]} = -0.0065$. In the perpendicular ([1$\bar{1}$0]) direction, the higher number of coincidence lattice sites ($1 \times d_{Sb[1\bar{1}0]}$ (3.72 Å) ≈ $2 \times d_{Cu[001]}$ (3.60 Å)) with a deviation parameter of $f_{[1\bar{1}0]} = 0.033$), in addition to the fast diffusion along the [1$\bar{1}$0] direction and the high sticking probability at the low-energy steps along the [110] direction,[22] would accommodate anisotropic growth. For the actual alignment of nanostripes to occur, however, there must be a local covalent bonding relaxation in the Sb[1$\bar{1}$0] direction to achieve coherency. Under this condition, the epitaxial alignment of the (001) plane of α-Sb with the Cu-(100) surface would be fulfilled by the coincidence lattice sites through the thick back lines (Figure 4a). The residual misfit in the [110] direction is accommodated in the form of a coincidence lattice misfit dislocation that appears in a displacement of the nearest-neighbor coincidence lattice unit by a minimum of 3.6 Å in the Cu[0$\bar{1}$0] direction. The discontinuity of the coincidence lattice leads to the formation of an evenly separated array of ~1-nm-wide nanostripes with an atomic gap. The dangling bonds of the Sb atoms on the two sides of the nanostripes would be terminated by the adsorption of a species from the solution, an advantage of the electrolyte environment that could be a factor that makes the nanostripes stable. Similar arguments can be made to orient a nanostripe in a perpendicular direction along the surface. The nanostripes would elongate until two perpendicularly orientated nanostripes encounter each other as shown in Figure 4b.

A 2D array of nanostripes thus formed serves as the template for the vertical alignment of the nanostripes. A layer-by-layer epitaxy of the nanostripes can be achieved and is a characteristic of a layered structure of α-Sb. The gradual release of strains

along the nanostripes, which would ensure the growth of nanostripes to form a 3D architecture without breaking down basic nanostripe features, is expected.

In summary, this study presents, for the first time, the formation of a nanostripe array with size confinement down to the scale of a few nanometers and 3D epitaxy stacking. Although the study provides an understanding of the growth of a semimetallic element, it can also be exploited as a model for other 3D nanostructures or alloy nanostructures using an as-formed nanostripe "array" as well as an "atomic gap" as templates.

Acknowledgment. This work was supported by the NSF of China (grant nos. 20021002, 20273056, 2001CB61050, and 29973040). We thank S. B. Yao for valuable discussions and Y. L. Chow for careful English improvements.

Supporting Information Available: Extensive in situ STM figures. This material is available free of charge via the Internet at http://pubs.acs.org.

References and Notes

(1) Miguel, J. J. de; Miranda, R. *J. Phys.: Condens. Matter* **2002**, *14*, R1063.
(2) Zhang, Z.; Lagally, M. G. *Science* **1997**, *276*, 377.
(3) Fruchart, O.; Klaua, M.; Barthel, J.; Kirschner, J. *Phys. Rev. Lett.* **1999**, *83*, 2769.
(4) Marcus, D. Lay; Stickney, J. L. *J. Am Chem. Soc.* **2003**, *125*, 1352.
(5) Teichert, C. *Phys. Rep.* **2002**, *365*, 335.
(6) Xia, Y. *Adv. Mater.* **2001**, *13*, 369.
(7) Vrijmoeth, J.; Vandervegt, H. A.; Meyer, J. A.; Vlieg, E.; Behm, R. J. *Phys. Rev. Lett.* **1994**, *72*, 3843.
(8) Parsons R.; Vandernoot T. *J. Electroanal. Chem.* **1988**, *257*, 9.
(9) Biefeld, R. M. *Mater. Sci. Eng., R* **2002**, *36*, 105.
(10) Prieto, A. L.; Martín-González, M.; Keyani, J.; Gronsky, R.; Sands, T.; Stacy, A. M. *J. Am. Chem. Soc.* **2003**, *125*, 2388.
(11) Hwang, R. Q.; Maria, C. B. *Chem. Rev.* **1997**, *97*, 1063.
(12) Kaiser, B.; Stegemann, B.; Kaukel, H.; Rademann, K. *Surf. Sci.* **2002**, *496*, L18.
(13) Wu, Q.; Shang, W. H.; Yan, J. W.; Xie, Z. X.; Mao, B. W. *J. Phys. Chem. B* **2003**, *107*, 4065.
(14) Ward, L. C.; Stickney, J. L. *Phys. Chem. Chem. Phys.* **2001**, *3*, 3364.
(15) Kolb, D. M. *Angew. Chem., Int. Ed.* **2001**, *40*, 1162.
(16) Wu, Q.; Shang, W. H.; Yan, J. W.; Mao, B. W. *J. Mol. Catal. A: Chem.* **2003**, *199*, 49.
(17) Dawson, J. L.; Wilkinson, J.; Gillibrand, M. I. *J. Inorg. Nucl. Chem.* **1970**, *32*, 501.
(18) Sorenson, T. A.; Sugg, D. W.; Nandhakumar, I.; Stickney, J. L. *J. Electroanal. Chem.* **1999**, *467*, 270.
(19) Günther, C.; Vrijmoeth, J.; Hwang, R. Q.; Behm, R. J. *Phys. Rev. Lett.* **1995**, *74*, 754.
(20) Trampert, A.; Ploog, K. H. *Cryst. Res. Technol.* **2000**, *35*, 793.
(21) Palmstrom C. J. *Annu. Rev. Mater. Sci.* **1995**, *25*, 389.
(22) Heller, E. J.; Lagally, M. G. *Appl. Phys. Lett.* **1992**, *60*, 2675.